

PRL-TR-3108

Best Available Copy

(2)

DTIC FILE COPY

TECHNICAL REPORT PRL-TR-3108

BRL

AD-A224 353

EFFECT OF ELECTROMAGNETIC FIELDS ON
THE STABILITY OF A PERFECTLY CONDUCTING,
AXISYMMETRIC SHAPED-CHARGE JET

S DTIC
ELECTE
JUL 25 1990 D
D Cg D

JOHN D. POWELL
DAVID L. LITTLEFIELD

JUNE 1990

APPROVED FOR PUBLIC RELEASE; DISTRIBUTION UNLIMITED.

20030206026

U.S. ARMY LABORATORY COMMAND

BALLISTIC RESEARCH LABORATORY
ABERDEEN PROVING GROUND, MARYLAND

3 1 24 037

NOTICES

Destroy this report when it is no longer needed. DO NOT return it to the originator.

Additional copies of this report may be obtained from the National Technical Information Service, U.S. Department of Commerce, 5285 Port Royal Road, Springfield, VA 22161.

The findings of this report are not to be construed as an official Department of the Army position, unless so designated by other authorized documents.

The use of trade names or manufacturers' names in this report does not constitute endorsement of any commercial product.

UNCLASSIFIED

REPORT DOCUMENTATION PAGE			Form Approved OMB No. O-104-0168
This form contains neither recommendations nor conclusions of the Defense Technical Information Center. It has been reviewed and approved for public release by the Defense Technical Information Center. Distribution outside DOD may require additional approval.			
1. AGENCY USE ONLY (Leave Blank)	2. REPORT DATE	3. REPORT TYPE AND DATES COVERED	
	June 1990	Final, Jan 89-Sep 89	
4. TITLE AND SUBTITLE		5. FUNDING NUMBERS	
Effect of Electromagnetic Fields on The Stability of a Perfectly Conducting, Axisymmetric Shaped-Charge Jet		PE: 61102A PR: 1L161102AH43 TA: 00 WU: 001 AJ	
6. AUTHOR(S)		7. PERFORMING ORGANIZATION NAME(S) AND ADDRESS(ES)	
John D. Powell and David L. Littlefield		8. PERFORMING ORGANIZATION REPORT NUMBER	
9. SPONSORING/MONITORING AGENCY NAME(S) AND ADDRESS(ES)		10. SPONSORING/MONITORING AGENCY REPORT NUMBER	
US Army Ballistic Research Laboratory ATTN: SLCBR-DD-T Aberdeen Proving Ground, MD 21005-5066		BRL-TR-3108	
11. SUPPLEMENTARY NOTES We thank D. Eccleshall and M.L. Lampson for their careful review and worthwhile suggestions about this manuscript, C.E. Hollandsworth and C.R. Hummer for discussions of electromagnetic field effects on shaped-charge jets, and E.H. Walker and J.T. Harrison for discussions on shaped-charge jet properties.		12a. DISTRIBUTION AVAILABILITY STATEMENT	
Approved for public release; distribution unlimited		12b. DISTRIBUTION CODE	
13. ABSTRACT (Maximum 250 words) <p>The stability characteristics of a shaped-charge jet which carries an electrical current are investigated. The jet is assumed to be perfectly plastic, perfectly conducting, and axisymmetric. The equations which govern the behavior of the jet are solved numerically using first-order perturbation theory, after the surface of the jet has been subjected to some arbitrary disturbance. The solution of these equations indicates that the jet is unstable. The growth rate of the instability depends upon the relative importance of inertial, electrical, and plastic forces, and upon the size of the disturbance wavelength relative to the jet radius. It is argued and demonstrated from the numerical solutions that the electromagnetic forces always make the jet more unstable than it would be in their absence. Application of the theory suggests that electromagnetic fields may be capable of enhancing jet breakup on a time scale of practical interest, but more work, both theoretical and experimental, needs to be done before definite conclusions can be drawn.</p>			
14. SUBJECT TERMS		15. NUMBER OF PAGES	
Shaped-Charge Jet, Metal Jet; Jet Stability, MHD Stability, Electromagnetic Disruption		25	
16. PRICE CODE			
17. SECURITY CLASSIFICATION OF REPORT	18. SECURITY CLASSIFICATION OF THIS PAGE	19. SECURITY CLASSIFICATION OF ABSTRACT	20. LIMITATION OF ABSTRACT
UNCLASSIFIED	UNCLASSIFIED	UNCLASSIFIED	UL

UNCLASSIFIED

INTENTIONALLY LEFT BLANK.

Table of Contents

	<u>Page</u>
LIST OF FIGURES	v
ACKNOWLEDGMENTS	vii
I. INTRODUCTION	1
II. MODEL AND GOVERNING EQUATIONS	3
III. ZERO-ORDER SOLUTION: IDEALIZED MOTION OF THE JET	6
IV. FIRST-ORDER EQUATIONS	8
V. SOLUTION OF FIRST-ORDER EQUATIONS AND STABILITY CHARACTERISTICS OF THE JET	11
VI. SUMMARY, CONCLUSIONS, AND FUTURE WORK	15
REFERENCES	17

INTENTIONALLY LEFT BLANK.

List of Figures

<u>Figure</u>		<u>Page</u>
1	Model for jet stability calculations.	3
2	Relative amplitude ω versus time for different values of K and with no electrical current present. The parameters A and H were given by 1.5 and zero, respectively.	13
3	Relative amplitude ω versus time for different values of K and with an electrical current present. The parameters A and H were given by 1.5 and 0.27, respectively.	14
4	Ratio of perturbed radius amplitudes for the current and no-current cases. The parameter A was given by 1.5	14
5	Relative amplitude ω versus time for current and no-current cases. The parameters A and K were given by 4.5 and $3\pi/4$, respectively.	16

Accession For	
NTIS CRA&I <input checked="" type="checkbox"/>	
DTIC TAB <input type="checkbox"/>	
Unannounced <input type="checkbox"/>	
Justification _____	
By _____	
Distribution / _____	
Availability Codes	
Dist	Avail and/or Special
A-1	



INTENTIONALLY LEFT BLANK.

ACKNOWLEDGMENTS

We wish to thank the following persons: D. Eccleshall and M. L. Lampson for carefully reviewing this manuscript and making a number of worthwhile suggestions; C. E. Hollandsworth and C. R. Hummer for numerous discussions concerning effects of electromagnetic fields on shaped-charge jets; and E. H. Walker and J. T. Harrison for discussions concerning the general properties of shaped- charge jets.

INTENTIONALLY LEFT BLANK.

I. INTRODUCTION

There has been speculation, since Walker's initial work¹ on the problem, that electromagnetic fields might be used effectively to destroy shaped-charge jets. Clearly if such an effect could be demonstrated conclusively, it would have enormous potential for military applications. The idea originally proposed by Walker was that large electric currents be used to vaporize the jet. It appears, however, that electromagnetic fields could be used in other ways as well, and it is important to assess the effectiveness of various physical mechanisms contributing to the destruction of the jet. In this report we will be concerned with one such mechanism, namely, how electromagnetic effects can increase the growth rate of instabilities which have been shown to occur even in the absence of these effects.

Metallic jets formed from explosive charges have been studied extensively. The basic theory governing their formation and propagation was developed many years ago in the well-known work of Birkhoff, MacDougall, Pugh, and Taylor² and, later, of Pugh, Eichelberger, and Rostoker.³ At least for a time after their formation, the jets are found to stretch as they propagate with a reasonably uniform velocity gradient across the length of the jet. Such a characteristic is highly desirable since the penetration capability of the jet increases with increasing length. Eventually, however, as radiographs have demonstrated, the jet will tend to neck down in places along its surface and finally break into segments.

This behavior suggested that the idealized stretching motion described above was not stable and has prompted a number of investigations into the stability characteristics of jets. Significant among these were the early one-dimensional investigations of Chou and Carleone,⁴ who concluded that perfectly plastic (no strain hardening) jets should be unconditionally unstable to perturbations along their surface. They identified a number of parameters which affected the growth rate of the instability and compared their results with computer simulations carried out by them and, earlier, by Karpp and Simon.⁵ These simulations were undertaken using Wilkins' two-dimensional, elastic-plastic HEMP code.⁶ Many effects seen in the simulations were predicted by the one-dimensional stability analysis. However, the simulations did suggest the existence of a critical or most unstable wavelength for the surface perturbation, as had also been supposed from analysis of the experimental data, and the one-dimensional stability calculations did not predict this effect. Presumably, this discrepancy led Carleone, Chou, and Ciccarelli⁷ to modify their model and account approximately for stress enhancement in the vicinity of the neck, an effect neglected in their earlier calculations. The revised version did predict a critical wavelength, although the value was not always in agreement with that observed in the simulations. Additional one-dimensional calculations, along similar lines, were later performed by Walsh.⁸ Using dimensional analysis, he identified a single parameter upon which the growth rate of the perturbation depended, and studied the time evolvement of jets with random initial surface disturbances.

In more recent work stability calculations have been extended to two dimensions by Frankel and Weihs,⁹ by Curtis,¹⁰ by Pack,¹¹ and by Romero.¹² The various investigations are all based on the assumption that the jet is axisymmetric and are differentiated primarily by the form of the constitutive relation assumed. The most satisfactory assumption seems to be that made by both Pack and Romero, in which the jet was taken to be perfectly

plastic and to satisfy the Levy-von Mises stress-strain relations. The work of Romero was particularly thorough. He identified a time-dependent parameter which measured essentially the ratio of inertial to plastic forces in the jet, and studied jet stability as a function of both that parameter as well as the structure of the perturbation. Most of the calculations were undertaken via numerical solutions of the linear differential equations which govern the time evolution of the perturbation, but some approximate limiting-case analytic solutions were also presented.

In this report we will follow basically the same general procedure used by Romero. We assume a perfectly plastic, shaped-charge jet which initially is stretching uniformly in the axial direction. Unlike in any previous work, however, we also assume that an electrical current is conducted along the surface of the jet. At time $t = 0$ the surface is subjected to a small perturbation so that its radius is no longer independent of the axial coordinate z . The equations of motion of the jet are then solved to determine how this perturbation evolves in time. As in previous work, we assume not only that the jet is axisymmetric initially, but restrict ourselves to perturbations which do not destroy the axial symmetry. Our principal interest lies in determining how electromagnetic fields associated with the current in the jet affect the growth times of instabilities which occur even in the absence of these electromagnetic effects.

A number of other assumptions are made in this first-effort calculation in order to make the analysis as tractable as possible. First, we assume as in Refs. 9 and 12 that the jet is infinitely long. In practice, this assumption means only that the dynamics of the tip and tail of the jet can be ignored, and implies that the analysis holds only at points well removed from the ends. This assumption seems reasonable because the length of the jet is large compared to its radius and, as will be seen, disturbances which grow appreciably have initial wavelengths which are smaller than or comparable to the initial radius the jet. Second, we have assumed that the jet is a perfect conductor. This assumption is strictly valid only if the magnetic Reynolds number¹³ associated with the jet is sufficiently large, a condition that is questionable for the case at hand. It is common, however, in stability calculations to assume infinite conductivity anyway, perhaps in the belief that the basic conclusions reached will not be significantly different from those obtained in the finite-conductivity case. In assuming infinite conductivity, we are in effect replacing $\vec{J} \times \vec{B}$ body forces by surface forces which result from current being carried only on the surface of the jet. We are also neglecting increases in the internal energy of the jet resulting from resistive heating. Consequently, we can expect the analysis to hold only for currents sufficiently low and times sufficiently short that large-scale changes in the energy, such as would produce melting, do not occur. These points will be further discussed in Secs. V and VI. Finally, we will neglect dissipation by plastic forces and assume that the jet is isothermal. Thus, we will not consider any energy-conservation equation in our analysis and this omission also facilitates the calculations.

The organization of the report is as follows. In Sec. II, we describe the model and indicate the basic equations assumed to govern the behavior of the jet. In Sec. III, the lowest-order solution to these equations is worked out. In Secs. IV and V, the first-order equations are derived and solved, and the stability characteristics of the jet discussed. Finally, Sec. VI contains our conclusions and plans for future work.

II. MODEL AND GOVERNING EQUATIONS

Consider a metallic, perfectly plastic, shaped-charge jet such as shown in Fig.1. The jet is infinitely extended in the z direction and is assumed to be symmetric about the z axis. The radius of the jet at any point is denoted by $r_b(z, t)$ and the unit normal to the jet surface at that point by \hat{n} . An electrical current $I(t)$ is supplied to the jet by an external power supply, and this current will produce electric and magnetic fields both inside the jet and in the vacuum which surrounds it. Though the analysis does not require that I be constant, we will make this assumption in the remainder of the report.

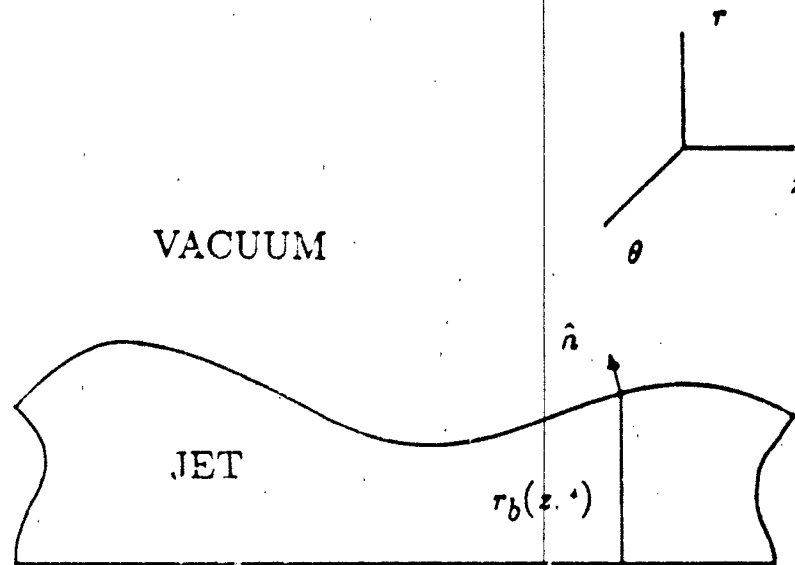


Figure 1. Model for jet stability calculations.

Let ρ and \vec{v} denote the density and material velocity in the jet. Let $\sigma_{\alpha\beta}$ denote an element of the stress tensor (a diagonal element is sometimes denoted by a single subscript) and let Y denote the yield stress. Let \vec{B} , \vec{E} , and \vec{J} denote the magnetic-induction field, the electric-field intensity, and the current density. Let σ be the electrical conductivity of the material composing the jet and μ be the free-space magnetic permeability. To accord with symmetry assumptions discussed above, we take $E_\theta = 0$, $J_\theta = 0$, $\vec{B} = B \hat{a}_\theta$, $\sigma_{\alpha\beta} = \sigma_{\alpha\beta} = 0$, and assume that the only nonvanishing components of \vec{v} are the r component u and the z component w .

The equations which govern the behavior of the interior of the jet are then taken to be¹⁴

$$\rho \frac{\partial u}{\partial t} + \rho u \frac{\partial u}{\partial r} + \rho w \frac{\partial u}{\partial z} = \frac{\partial \sigma_r}{\partial r} + \frac{\sigma_r - \sigma_\theta}{r} + \frac{\partial \sigma_{rz}}{\partial z} - J_z B \quad (1)$$

$$\rho \frac{\partial w}{\partial t} + \rho u \frac{\partial w}{\partial r} + \rho w \frac{\partial w}{\partial z} = \frac{\partial \sigma_z}{\partial z} + \frac{\partial \sigma_{rz}}{\partial r} + \frac{\sigma_{rz}}{r} + J_r B \quad (2)$$

$$\frac{\partial u}{\partial r} + \frac{u}{r} + \frac{\partial w}{\partial z} = 0 \quad (3)$$

$$\frac{\partial u}{\partial r} = \nu(2\sigma_r - \sigma_\theta - \sigma_z) \quad (4)$$

$$\frac{u}{r} = \nu(2\sigma_\theta - \sigma_r - \sigma_z) \quad (5)$$

$$\frac{\partial u}{\partial z} + \frac{\partial w}{\partial r} = 6\nu\sigma_{rz} \quad (6)$$

$$(\sigma_r - \sigma_\theta)^2 + (\sigma_\theta - \sigma_z)^2 + (\sigma_z - \sigma_r)^2 + 6\sigma_{rz}^2 = 2Y^2 \quad (7)$$

$$\mu J_r = -\frac{\partial B}{\partial z} \quad (8)$$

$$\mu J_\theta = \frac{1}{r} \frac{\partial}{\partial r} (rB) \quad (9)$$

$$\frac{\partial B}{\partial t} = \frac{\partial E_r}{\partial r} - \frac{\partial E_\theta}{\partial z} \quad (10)$$

$$J_r = \sigma(E_r - uB) \quad (11)$$

$$J_\theta = \sigma(E_\theta + uB). \quad (12)$$

These equations have the following meanings. Equations (1)-(3) express conservation of momentum and mass. The jet has been assumed to be incompressible so that mass conservation takes the simple form represented by Eq.(3). The last term on the right-hand of both Eqs.(1) and (2) represents the Lorentz force. The jet is assumed to be electrically neutral so that electrostatic forces need not be included in these equations and, in fact, any other external forces are taken to be negligible. Equations (4)-(7) are the standard equations which govern the motion of a perfectly plastic axisymmetric material in cylindrical coordinates, with Eq. (4)-(6) representing the Levy-von Mises stress-strain relations and Eq.(7) the von Mises yield condition. The parameter ν is a time-dependent factor which must be determined in the analysis. Equations (8)-(10) are Maxwell's equations. The displacement current has been neglected in Eq. (10); in general, including this term produces only terms of the order of v/c , where v is a typical velocity in the jet and c is the

light speed. Consequently, the effect of this current is clearly negligible for the problem at hand. Equations (11) and (12) represent Ohm's law for the two nonvanishing components of the current density.

In the vacuum surrounding the jet, i.e., for $r > r_b$, Eqs. (3)-(7) are meaningless, but the remaining equations hold with $\rho = 0$, $\vec{J} = 0$, and $\sigma_{\alpha\beta} = 0$. These equations therefore imply certain boundary conditions that must exist at the interface between the jet and the vacuum. The appropriate conditions can be obtained by integrating each of the relevant equations across the boundary, of assumed thickness δ , in a direction normal to the surface and then taking the limit as $\delta \rightarrow 0$. Let \hat{n} be the unit normal to the separating surface pointing in the positive radial direction and let $d\ell$ be an element of arc length normal to the surface. Following the procedure discussed elsewhere,¹⁸ we now multiply each of the pertinent equations through by $d\ell$ and integrate across the boundary. We allow for a surface current j^* so that the integral of \vec{J} produces j^* as $\delta \rightarrow 0$. Finally, we observe that the integral of each partial time-derivative, $\frac{\partial F}{\partial t}$, produces, except for terms which vanish with δ , the result $-\vec{v} \cdot \hat{n} < F >$. The brackets here denote the change in F as the boundary is crossed.

The following results are obtained when the integrations above are carried out. After we make use of Eqs.(8) and (9), the integrals of Eqs. (1) and (2) yield

$$<\sigma_r>n_r + <\sigma_{rr}>n_r = \frac{1}{2\mu} < B^2 > n_r, \quad (13)$$

and

$$<\sigma_s>n_s + <\sigma_{rs}>n_s = \frac{1}{2\mu} < B^2 > n_s; \quad (14)$$

equations (8) and (9) yield

$$\mu j_r^* = - < B > n_r, \quad (15)$$

and

$$\mu j_s^* = < B > n_s; \quad (16)$$

equation (10) yields

$$- < B > \vec{v} \cdot \hat{n} = < E_r > n_r - < E_s > n_s. \quad (17)$$

Equations (11) and (12) yield $j^* = 0$ unless σ is infinite in which case they yield no information. We finally observe that since the boundary moves with the jet, we must have

$$\frac{dr_b}{dt} = \frac{\partial r_b}{\partial t} + w \frac{\partial r_b}{\partial z} = u, \quad \text{at } r = r_b \quad (18)$$

and that the unit normal \hat{n} is given by

$$\hat{n} = \frac{\hat{a}_r - \frac{\partial r}{\partial z} \hat{a}_z}{[1 + (\frac{\partial r}{\partial z})^2]^{1/2}}. \quad (19)$$

This system of twelve equations and appropriate boundary conditions are sufficient in principle to completely specify the motion of the jet or, alternatively, to determine as a function of position and time the twelve unknowns: u , w , σ_r , σ_z , σ_{rz} , σ_{zz} , v , E_r , E_z , J_r , J_z , and B . The equations are obviously difficult to solve in general, and we will be interested in simplifying them by undertaking a linear perturbation solution. Through such a solution it is possible to study the stability of the motion of the jet to various types of perturbations in a comparatively simple way. Furthermore, as will be seen, it is sometimes possible to solve only a subset of the available equations, the remaining ones being necessary to determine properties of the jet which do not affect the stability analysis.

III. ZERO-ORDER SOLUTION: IDEALIZED MOTION OF THE JET

Experimental studies in the motion of shaped-charge jets have indicated that at early times the jets stretch rather uniformly as they propagate, with the jet radius being independent of z and the velocity w increasing linearly across the length of the jet. At later times there appear along the surface of the jet perturbations which tend to disrupt this idealized motion. The purpose of stability analysis is to determine whether these perturbations grow in time and, if so, how rapidly.

In order to study jet stability in the presence of electromagnetic fields, we will assume the same basic type of idealized motion at early times. Thus we take r_0 independent of z and $w = A(t)z$, where $A(t)$ is to be determined. As indicated previously, it will also be assumed in this first analysis that the jet is perfectly conducting (σ infinite) and that the current I is carried along the outer surface, i. e., at $r = r_0$. We take the initial strain rate to be β (assumed given), the initial radius to be r_0 , and denote by subscript zero the lowest-order solution to the governing equations, i. e. the solution which represents the idealized motion. The superscript V is used hereafter to denote the value of some quantity in the vacuum, whereas the absence of a superscript denotes the value in the jet. The origin of the coordinate system can be chosen arbitrarily and we take one which moves with the center of mass of the jet. Thus, w in the governing equations means the velocity relative to the center of mass and $w = 0$ at $z = 0$.

According to the assumptions above and from Ampere's law, it follows that in the jet $\vec{J}_0 = 0$ and $B_0 = 0$, while in the vacuum

$$B_0^V = \frac{\mu I}{2\pi r}. \quad (20)$$

Finally, since $n_{r,0} = 1$ and $n_{z,0} = 0$, we conclude from the boundary conditions in (15) and (16) that

Table 1. Solution of Governing Equations in Zero-Order.

Jet	Vacuum	Surface
$w_0 = \gamma\beta z$	$B_0^V = \frac{\mu I}{2\pi r}$	$n_{r,0} = 1$
$u_0 = -\gamma\beta r/2$		$n_{z,0} = 0$
$r_{b,0} = \gamma^{1/2}r_0$		$j_r^* = 0$
$\sigma_{r,0} = \frac{3\beta\beta^2\gamma^2}{8}(r^2 - \gamma r_0^2) - \frac{\mu I^2}{8\pi^2 r_0^2 \gamma}$		$j_z^* = \frac{I}{2\pi r_0 \gamma^{1/2}}$
$\sigma_{z,0} = Y + \frac{3\beta\beta^2\gamma^2}{8}(r^2 - \gamma r_0^2) - \frac{\mu I^2}{8\pi^2 r_0^2 \gamma}$		
$\sigma_{\theta,0} = \frac{3\beta\beta^2\gamma^2}{8}(r^2 - \gamma r_0^2) - \frac{\mu I^2}{8\pi^2 r_0^2 \gamma}$		
$\sigma_{rz,0} = 0$		
$v_0 = \frac{r_0}{2Y}$		
$J_{r,0} = 0$		
$J_{z,0} = 0$		
$B_0 = 0$		

$$j_{z,0}^* = \frac{I}{2\pi r_{b,0}}, \quad (21)$$

and

$$j_{r,0}^* = 0. \quad (22)$$

The remaining fluid-mechanical properties of the jet in zero order follow by solving the equations of the preceding section under the assumptions discussed above. The analysis is similar to that which has been undertaken elsewhere^{11,12} and will not be repeated in detail here. The only significant difference with the nonelectrical case is that the stress components must satisfy the boundary conditions represented by (13) and (14), whereas for no magnetic fields the right-hand sides of these equations reduce to zero. Results of all zero-order quantities, except for the electric fields which are not needed in the subsequent analysis, are presented for reference in Table I. They can be seen by direct substitution to satisfy the equations and boundary conditions in Sec. II. In this table the parameter γ is given by

$$\gamma = \frac{1}{1 + \beta t}. \quad (23)$$

IV. FIRST-ORDER EQUATIONS

We now wish to consider the form taken by the equations of Sec.II in first-order perturbation theory. We therefore assume that each physical quantity can be represented by the zero-order solution plus a small correction, and linearize the governing equations about those corrections. Therefore, for each quantity F we assume

$$F \approx F_0 + F_1(r, z, t), \quad (24)$$

substitute in the equations of Sec.II, and retain only the terms which are of order F_1 or lower. The solution of the first-order equations should then predict the stability of the jet to the idealized motion described in the preceding section.

Considering first just the fluid-mechanical equations in the jet, we find after making the substitution above in Eqs.(1)-(7), that the resulting equations can be partly uncoupled to produce

$$\rho \frac{\partial u_1}{\partial t} + \rho u_1 \frac{\partial u_0}{\partial r} + \rho u_0 \frac{\partial u_1}{\partial r} + \rho w_0 \frac{\partial u_1}{\partial z} = \frac{\partial \sigma_{s,1}}{\partial r} + \frac{1}{6\nu_0} \frac{\partial^2 u_1}{\partial z^2} \quad (25)$$

$$\rho \frac{\partial w_1}{\partial t} + \rho u_0 \frac{\partial w_1}{\partial r} + \rho w_1 \frac{\partial w_0}{\partial z} + \rho w_0 \frac{\partial w_1}{\partial z} = \frac{\partial \sigma_{s,1}}{\partial z} + \frac{1}{6\nu_0} \left[\frac{\partial^2 w_1}{\partial r^2} + \frac{1}{r} \frac{\partial w_1}{\partial r} - \frac{\partial^2 w_1}{\partial z^2} \right] \quad (26)$$

and

$$\frac{\partial u_1}{\partial r} + \frac{u_1}{r} + \frac{\partial w_1}{\partial z} = 0. \quad (27)$$

Similarly, the electromagnetic equations, (8)-(12), can be uncoupled to yield a single result which describes the convection of the induction field in the jet, namely,

$$\frac{\partial B_1}{\partial t} + \frac{\partial u_0}{\partial r} B_1 + u_0 \frac{\partial B_1}{\partial r} + w_0 \frac{\partial B_1}{\partial z} + \frac{\partial w_0}{\partial z} B_1 = 0. \quad (28)$$

The results from Table I are to be used to obtain the zero-order functions.

In the vacuum it seems that there can be no perturbation to the existing induction field. This conclusion follows most directly from Ampere's law and the assumed symmetry of the problem. That is, since there is only an azimuthal component of \vec{B} and this component is independent of angle, the induction field is given to all orders by Eq. (20) and we have

$$B_1^V = 0. \quad (29)$$

As indicated before, we will find no need in this problem to calculate the first-order electric fields in the vacuum, provided we restrict ourselves to studying the stability properties of the jet.

Finally, we consider the boundary conditions in first order. Evidently, we have from Eq.(19)

$$\vec{n}_1 = -\frac{\partial r_{b,1}}{\partial z} \hat{a}_z. \quad (30)$$

Other first-order quantities evaluated at the boundary are, in accordance with standard procedure, represented by their Taylor expansion about $r = r_{b,0}$. Consequently, for any F we have through first order

$$F(r_b) = F_0(r_{b,0}) + F_1(r_{b,0}) + \left(\frac{\partial F_0}{\partial r}\right)_{r_{b,0}} r_{b,1}. \quad (31)$$

We now use Eq.(31) and the results in Table I to evaluate the boundary condition represented by Eq.(13). We find

$$\sigma_{z,1}(r_{b,0}) = \left[\frac{\mu I^2}{4\pi^2 \gamma^{3/2} r_0^3} - \frac{3\rho\beta^2\gamma^{5/2}r_0}{4} \right] r_{b,1} - \frac{Y}{3\gamma\beta} \left[\left(\frac{\partial u_1}{\partial r} \right)_{r_{b,0}} - \frac{u_1(r_{b,0})}{r_{b,0}} \right]. \quad (32)$$

In obtaining this result we have used the expression

$$\frac{\partial u_1}{\partial r} - \frac{u_1}{r} = 6\nu_0(\sigma_{r,1} - \sigma_{z,1}), \quad (33)$$

easily derived from the linearized versions of (4),(5), and (7), to express $\sigma_{r,1}$ in terms of $\sigma_{z,1}$ and u_1 . Similarly, from Eq. (14) and the linearized version of (6), we have

$$\frac{1}{3\gamma\beta} \left[\left(\frac{\partial u_1}{\partial z} \right)_{r_{b,0}} + \left(\frac{\partial w_1}{\partial r} \right)_{r_{b,0}} \right] = \frac{\partial r_{b,1}}{\partial z}. \quad (34)$$

Finally, we have from (18) in first order

$$\frac{\partial r_{b,1}}{\partial t} + \gamma\beta z \frac{\partial r_{b,1}}{\partial z} = u_1(r_{b,0}) - \frac{\gamma\beta}{2} r_{b,1}. \quad (35)$$

The remaining conditions, those implied in (15)-(17), need not be considered in the subsequent analysis.

We now observe that Eqs. (25),(26), and (27) along with the boundary conditions represented by (32), (34), and (35) are sufficient to determine the quantities u_1 , w_1 , $\sigma_{z,1}$, and $r_{b,1}$ for all time, given some set of initial conditions. As will be seen these results are sufficient to study the stability of the jet.

It is convenient for further analysis to follow the basic procedure of Romero¹² and perform a transformation which removes the explicit z dependence from the governing equations. Consequently, we define new coordinates

$$\xi = \frac{\gamma z}{r_0} \quad \eta = \frac{r}{r_0 \gamma^{1/2}} \quad (36)$$

and substitute into Eqs. (25), (26), (27), (32), (34), and (35). Since the results now contain no explicit dependence on ξ , the solution of the equations can be taken to be of the form

$$\begin{aligned} u_1(\eta, \xi, \tau) &= \beta r_0 \tilde{u}_1(\eta, \tau) e^{iK\xi} \\ w_1(\eta, \xi, \tau) &= \beta r_0 \tilde{w}_1(\eta, \tau) e^{iK\xi} \\ \sigma_{z,1}(\eta, \xi, \tau) &= Y \tilde{\sigma}_{z,1}(\eta, \tau) e^{iK\xi} \\ r_{b,1}(\xi, \tau) &= r_0 \tilde{r}_{b,1}(\tau) e^{iK\xi}. \end{aligned} \quad (37)$$

Here K is a dimensionless wave number, related to the real wave number k through the relation

$$K = r_0 k = \frac{2\pi r_0}{\lambda_0}, \quad (38)$$

where λ_0 is the initial wavelength of the perturbation. We have also normalized the velocities by βr_0 , the stress by Y , the jet radius by r_0 , and defined a dimensionless time τ given by

$$\tau = \beta t. \quad (39)$$

Using these results in Eqs. (25), (26), (27), (32), (34), and (35), we find that the dimensionless first-order variables must satisfy the following set of equations

$$\frac{\partial \tilde{w}_1}{\partial \tau} + \gamma \tilde{w}_1 = iAK\gamma \tilde{\sigma}_{z,1} + \frac{A}{3\gamma^2} \left[\frac{\partial^2 \tilde{w}_1}{\partial \eta^2} + \frac{1}{\eta} \frac{\partial \tilde{w}_1}{\partial \eta} + \gamma^3 K^2 \tilde{w}_1 \right], \quad (40)$$

$$\frac{\partial \tilde{u}_1}{\partial \eta} + \frac{\tilde{u}_1}{\eta} + i\gamma^{3/2} K \tilde{w}_1 = 0, \quad (41)$$

and

$$\frac{\partial^2 \tilde{\sigma}_{z,1}}{\partial \eta^2} + \frac{1}{\eta} \frac{\partial \tilde{\sigma}_{z,1}}{\partial \eta} - \gamma^3 K^2 \tilde{\sigma}_{z,1} = -\frac{iK}{3} \left[\frac{\partial^2 \tilde{w}_1}{\partial \eta^2} + \frac{1}{\eta} \frac{\partial \tilde{w}_1}{\partial \eta} + \gamma^3 (2K^2 - 9/A) \tilde{w}_1 \right], \quad (42)$$

with boundary conditions

$$\tilde{\sigma}_{1,s}(\eta = 1) = \frac{3\gamma^{5/2}}{4A} [H/\gamma^4 - 1] \tilde{r}_{b,1} - \frac{1}{3\gamma^{3/2}} [(\frac{\partial \tilde{u}_1}{\partial \eta})_{\eta=1} - \tilde{u}_1(\eta = 1)], \quad (43)$$

$$\frac{iK}{3\gamma} \tilde{u}_1(\eta = 1) + \frac{1}{3\gamma^{5/2}} (\frac{\partial \tilde{w}_1}{\partial \eta})_{\eta=1} = iK \tilde{r}_{b,1}, \quad (44)$$

and

$$\frac{\partial \tilde{r}_{b,1}}{\partial \tau} = \tilde{u}_1(\eta = 1) - \frac{\gamma}{2} \tilde{r}_{b,1}. \quad (45)$$

In obtaining these results, we have combined Eqs.(25) and (27) to produce, instead of (25), a Poisson-type, second-order equation for the stress represented by Eq.(42). The result is obtained by differentiating (27) with respect to t , (25) with respect to r , and combining results. This form of the equation is particularly amenable to numerical solution.

The dimensionless parameters A and H in the above equations are defined by

$$A = \frac{Y}{\rho r_0^2 \beta^2}, \quad (46)$$

and

$$H = \frac{\mu I^2}{3\pi^2 \rho r_0^4 \beta^2}. \quad (47)$$

V. SOLUTION OF FIRST-ORDER EQUATIONS AND STABILITY CHARACTERISTICS OF THE JET

We now proceed to solve Eqs. (40)-(45) of the preceding section and thereby to study the stability characteristics of the jet as a function of the dimensionless parameters A , H , and K . Physically, A and H measure, respectively, the importance of plastic and electrical forces relative to inertial forces, and K is a measure of the size of the initial wavelength of the perturbation relative to the initial radius of the jet. It is noteworthy that the parameter H , and thus all electrical effects, occurs only in the boundary condition represented by Eq.(43). This rather special dependence is a consequence of our assumptions of infinite conductivity and axial symmetry. As will be seen in the following analysis, however, this one term can have a marked effect.

Before the equations can be solved we must first specify a set of initial conditions. Apparently, one need only specify $\tilde{w}_1(\eta, \tau = 0)$ since the remaining conditions, namely, those on \tilde{u}_1 , $\tilde{r}_{b,1}$, and $\tilde{\sigma}_{z,1}$, then follow from Eqs.(41), (44), and (43), respectively. In the remainder of the analysis we restrict ourselves to initial values of \tilde{w}_1 which are constant and denoted by iC where C is real. Solving the equations noted above then yields

$$\bar{u}_1(\eta, \tau = 0) = \frac{CK\eta}{2}, \quad (48)$$

$$\bar{r}_{b,1}(\tau = 0) = \frac{CK}{6}, \quad (49)$$

and

$$\tilde{\sigma}_{z,1}(\eta, \tau = 0) = \left[\frac{KC}{8A}(H - 1) + (2K^2 - 9/A) \frac{C}{3K} \right] \frac{I_0(K\eta)}{I_0(K)} - (2K^2 - 9/A) \frac{C}{3K} \quad (50)$$

where I_0 is a modified Bessel function. The constant C can be chosen arbitrarily and we take $C = 6/K$ so that $\bar{r}_{b,1}(\tau = 0) = 1$.

To solve Eqs. (40)-(45), we have represented both time and space derivatives by finite differences and numerically solved the resulting set of linear algebraic equations by matrix inversion. The procedure is quite straightforward and need not be discussed here in detail. Typically, a time step $\Delta\tau$ of 0.005 and a grid spacing which depended on the wavelength of the initial perturbation was used. In general, small wavelengths require more grid points to achieve spatial resolution and we have, in some cases, used as many as 400. This point has been further discussed by Romero.¹²

In stability calculations in which there is explicit time dependence, it is customary to consider how the relative amplitude ω given by

$$\omega = \frac{|r_{b,1}|}{r_{b,0}} \quad (51)$$

varies with time. If this quantity grows monotonically the jet is assumed to be unstable, whereas if it remains constant or approaches some asymptotic value, the jet is stable. We therefore wish to consider this amplitude, obtained by solving the equations discussed previously, for several cases of interest.

Shown in Fig. 2 is ω as a function of τ for different values of the dimensionless parameter K . The parameters A and H were taken to be 1.5 and zero, respectively. The value of A is reasonable since this quantity is of order unity for typical shaped-charge jets and $H = 0$ corresponds, of course, to no electrical current present. For typical strain rates, each unit of dimensionless time corresponds in real time to a few tens of microseconds. As is evident for each value of K considered, ω continues to grow for the time plotted. Consequently, the jet is unstable regardless of the initial wavelength of the perturbation. The value $K = \pi$, which corresponds to a wavelength equal to the initial diameter of the jet, leads to the maximum initial growth rate for the various cases considered. The two shortest wavelengths, namely, those corresponding to $K = 2\pi$ and $K = 4\pi$ are nearly stable initially. However, their amplitudes begin to grow once the jet has stretched enough that the wavelength becomes comparable in size to the jet diameter. At that time the

amplitude grows very rapidly, eventually becoming larger than the amplitude of the longer-wavelength perturbations which had high initial growth rates. For the two long-wavelength modes considered, corresponding to K given by $\pi/2$ and $\pi/8$, the growth rate decreases with increasing wavelength. These results are in basic agreement with the conclusions reached by Romero.¹²

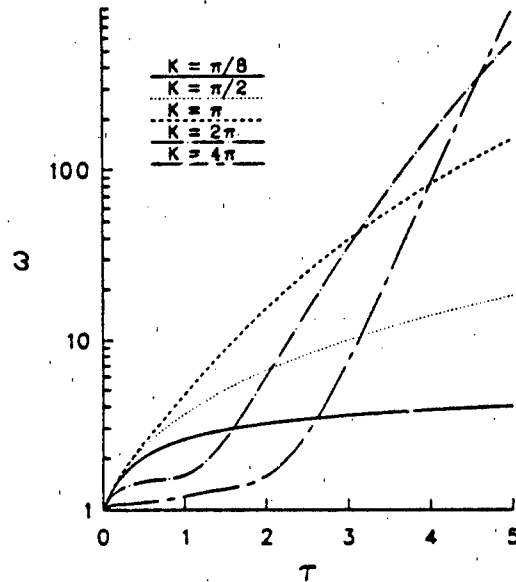


Figure 2. Relative amplitude ω versus time for different values of K and with no electrical current present. The parameters A and H were given by 1.5 and zero, respectively.

The corresponding cases for $H \neq 0$, i.e., for an electrical current present, are shown in Fig. 3. For currents of the order of 100 kA or so, the parameter H is also of the order of unity for typical jets. For the cases plotted in the figure, H was actually taken to be somewhat smaller, namely, 0.27. Apparently, the current produces no change in the basic shapes of the curves or in the qualitative conclusions reached for the no-current case. It is evident, however, that the current does produce an increase in the relative amplitude at any given time for all the wavelengths considered. This effect can be seen most easily in Fig. 4 in which the ratio $\omega_{H \neq 0}/\omega_{H=0}$, with appropriate values of ω taken from Figs. 2 and 3, is plotted for each value of K . Clearly this ratio corresponds to the ratio of the perturbed radius amplitude, $\tilde{r}_{b,1}$, in the current and no-current cases. Evidently, the overall effect of the electrical current is to enhance the instability.

Our qualitative understanding of this instability and of the behavior exhibited in Figs. 2 and 3 can be described approximately as follows. When the jet begins to neck down in some localized region, there is a tendency for the material on the right-hand side of the neck minimum to be accelerated toward regions of increasing cross sectional area, and to be decelerated on the opposite side. If there were no change in the stress, then, the mass in the neck would be decreased still more, resulting in unconditional instability. In reality, however, the longitudinal stress in the vicinity of the neck is, on the average, increased by an

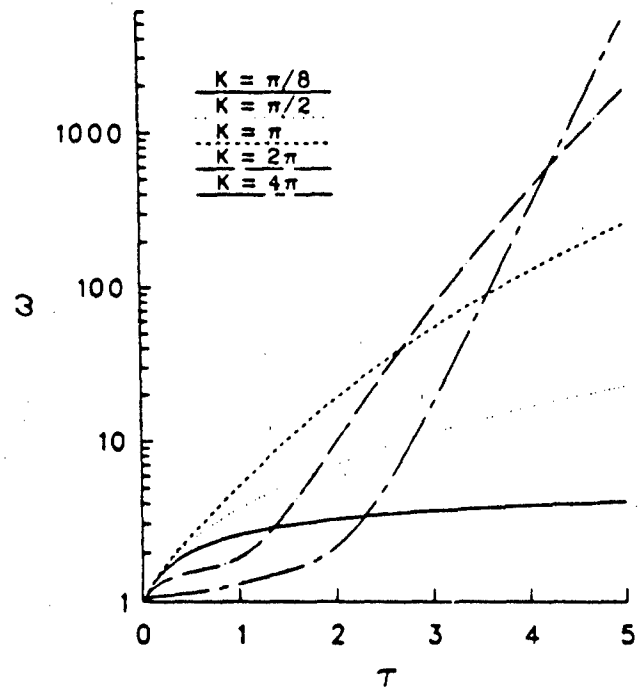


Figure 3. Relative amplitude ω versus time for different values of K and with an electrical current present. The parameters A and H were given by 1.5 and 0.27, respectively.

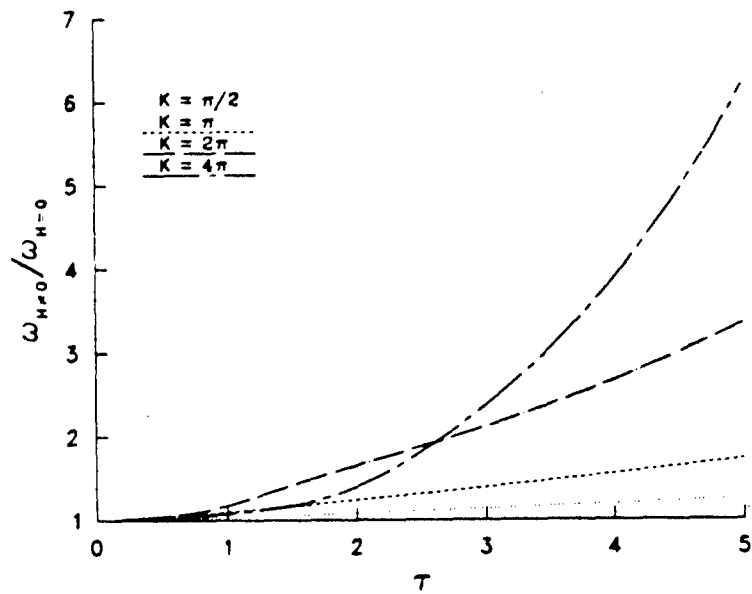


Figure 4. Ratio of perturbed radius amplitudes for the current and no-current cases. The parameter A was given by 1.5

amount which increases with increasing curvature of the surface or decreasing wavelength of the perturbation. Since the material prefers to flow from regions of low stress to regions of high stress, this enhancement tends to cause flow back into neck and produce a stabilizing effect. For sufficiently short wavelengths, near stability can result. The wavelength does, however, increase with time because the material is stretching and perturbations which are almost stable initially eventually become very unstable. For extremely long-wavelength disturbances, the perturbation is hardly felt in local regions of the jet. Consequently, the growth rate of the instability decreases with increasing wavelength, with the jet eventually becoming neutral to all perturbations in the infinite wavelength limit. When a current is added, the current must flow down the left-hand side of the neck and back up the right-hand side. The axial component of the Lorentz force associated with this current points in the positive z direction on the right and in the negative z direction on the left. The effect of the current therefore is to accelerate material out the neck, always increasing the perturbation and enhancing the instability.

In practical applications of electromagnetic forces to shaped-charge jets, it is likely that the current will be applied at some distance from where the jet is initially formed. Obviously the point of these calculations has not been to simulate realistically the details of such an occurrence but, rather, to examine how the current affects the general stability characteristics of the jet. Some estimate of the response of the jet subsequent to current initiation can be obtained from the foregoing theory, however, by taking for the initial strain rate β and initial radius r_0 values appropriate for the jet when the current is initiated. These values are somewhat smaller than the real initial values. It is then implicitly assumed that prior to current initiation the surface of the jet is negligibly disturbed.

To undertake such a calculation we considered a copper jet similar to that discussed in Ref. 11, and assumed that the current was applied when the radius of the jet was 2 mm. A simple calculation then revealed that the strain rate at that time was about $2.5 \times 10^4 \text{ s}^{-1}$. Other parameters taken in the calculation were $\rho = 8.9 \times 10^3 \text{ kg/m}^3$ and $Y = 100 \text{ MPa}$, and a current I of 150 kA was assumed. We then found from Eqs. (46) and (47) that $A \approx 4.5$ and $H \approx 10.7$. Results of the numerical solution of Equations (40)-(45) for these parameters are shown in Fig. 5 where ω is plotted versus the real time t for both the current and no current ($H=0$) cases. The dimensionless wavelength K was taken to be $3\pi/4$, a value reasonably close to the most unstable one. The electromagnetic forces obviously produce quite a remarkable increase (more than a factor of two) in disturbance amplitude in the fairly short time of about $25\mu\text{s}$. It seems reasonable to expect therefore that these forces could contribute significantly to the breakup time of the jet. We should also point out the assumed current is fairly modest and is not expected to produce large-scale heating of the jet during this time period.

VI. SUMMARY, CONCLUSIONS, AND FUTURE WORK

We have developed a model and undertaken calculations to examine the effects of electromagnetic forces on the stability of a perfectly conducting shaped-charge jet. Basic conclusions reached as a result of this study can be summarized as follows: (1). In general,

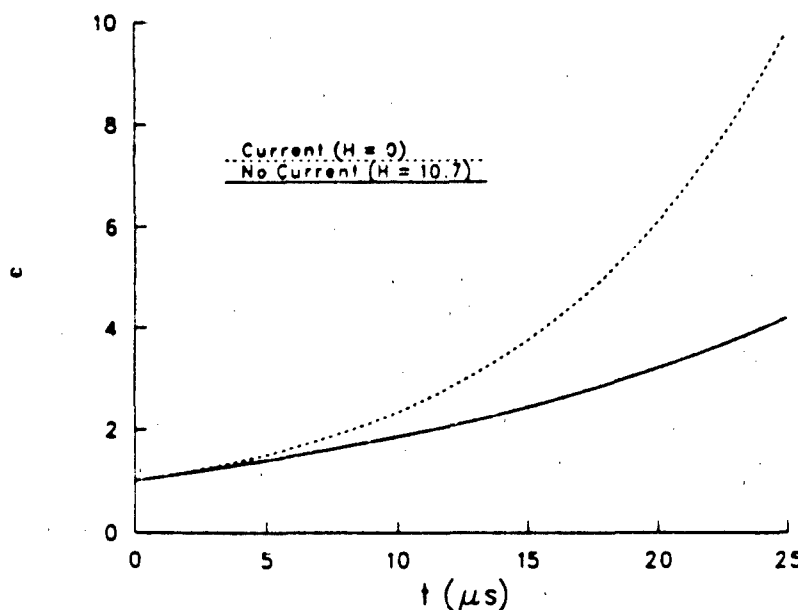


Figure 5. Relative amplitude ω versus time for current and no-current cases. The parameters A and K were given by 4.5 and $3\pi/4$, respectively.

the jets become more unstable as either of the dimensionless parameters A or H increases. The first parameter is a measure of the magnitude of plastic forces relative to inertial forces, and the second the magnitude of electrical forces relative to inertial forces. (2). The stability of the jet also depends on how the wavelength of the perturbation compares in size relative to the radius of the jet. Both the very short and the very long wavelengths are more stable than those of moderate magnitude, and there is a "critical" wavelength which produces maximum instability. (3). The stability properties of the jet vary with time because the jet stretches as it propagates. Thus, for example, as the jet radius decreases with increasing time, electrical effects become more and more important because of the increased induction field at the surface of the jet. (4). Many factors make the suitability of the calculations tenuous for computing in detail how electromagnetic fields will affect jet breakup time. However, what are thought to be reasonable estimates for the parameters involved lead to predictions that these forces should indeed produce a significant effect on a time scale of practical interest.

In the future it would be of interest to extend the above calculations to cases which do not preserve the axial symmetry, and to examine the effects of finite conductivity on the growth rates of the instabilities. The first of these problems is currently under investigation in house and the second is slated for future study. Obviously, it would also be beneficial to have some experimental data on jet disruption to compare with the theory. Some experimental work¹⁶ has already been carried out and it is hoped that more will be forthcoming in the near future.

References

1. Walker, E. H., "Defeat of Shaped Charge Devices by Active Armor," BRL Memorandum Report Number 2309, 1973.
2. Birkhoff, G., MacDougall, D. P., Pugh, E. M., and Taylor, G., J. Appl. Phys. 19, 563 (1948).
3. Pugh, E.M., Eichelberger, R.J., and Rostoker, N., J. Appl. Phys. 23, 532 (1952).
4. Chou, P.C., and Carleone, J., J. Appl. Phys. 48, 4187 (1977).
5. Karpp, R.P. and Simon, J., "An Estimate of the Strength of a Copper Shaped Charge Jet and the Effect of Strength on the Breakup of a Stretching Jet," US Army Ballistic Research Laboratory Report No. 1893, 1978.
6. Wilkins, M. L., in Methods in Computational Physics, edited by Alder, B., Fernbach, S., and Rotenberg, M. (Academic, New York, 1964), Vol.III, p. 211.
7. Carleone, J., Chou, P., and Ciccarelli, R. D., "Shaped Charge Jet Stability and Penetration Calculations," US Army Ballistic Research Laboratory Contract Report No. 351, 1977.
8. Walsh, J.M., J. Appl. Phys. 56, 1997 (1984).
9. Frankel, I. and Weihs D., J. Fluid Mech. 155, 289 (1985).
10. Curtis, J. P., J. Appl. Phys. 61, 4978 (1987).
11. Pack, D.C., J. Appl. Phys. 63, 1864 (1985).
12. Romero, L.A., J. Appl. Phys. 65, 3006 (1989).
13. See, e. g., Krall, N. A. and Trivelpiece, A. W., Principles of Plasma Physics (McGraw-Hill, New York, 1973), Chap. 3.
14. For the appropriate equations without EM fields, see, e.g., Hill, R., The Mathematical Theory of Plasticity (Oxford University Press, London, 1964), Chap. 10 or Ref. 11.
15. Kruskal, M. and Schwartzschild, M., Proc. R. Soc. London Ser. A 223, 348 (1954).
16. Lim, M. F. and Cayere, Paul, "Electromagnetic Armor Proof-of-Principle Test Program," Physics International Draft Report to DNA under Contract DNA001-87-C-01011, January 1988.

INTENTIONALLY LEFT BLANK.

No of Copies	Organization	No of Copies	Organization
1	Office of the Secretary of Defense OUSD(A) Director, Live Fire Testing ATTN: James F. O'Bryan Washington, DC 20301-3110	1	Director US Army Aviation Research and Technology Activity Ames Research Center Moffett Field, CA 94035-1099
2	Administrator Defense Technical Info Center ATTN: DTIC-DDA Cameron Station Alexandria, VA 22304-6145	1	Commander US Army Missile Command ATTN: AMSMI-RD-CS-R (DOC) Redstone Arsenal, AL 35898-5010
1	HQDA (SARD-TR) WASH DC 20310-0001	1	Commander US Army Tank-Automotive Command ATTN: AMSTA-TSL (Technical Library) Warren, MI 48397-5000
1	Commander US Army Materiel Command ATTN: AMCDRA-ST 5001 Eisenhower Avenue Alexandria, VA 22333-0001	1	Director US Army TRADOC Analysis Command ATTN: ATAA-SL White Sands Missile Range, NM 88002-5502
1	Commander US Army Laboratory Command ATTN: AMSLC-DL Edgewood, MD 20783-1145	(Class only) 1	Commandant US Army Infantry School ATTN: ATSH-CD (Security Mgr.) Fort Benning, GA 31905-5660
2	Commander US Army, ARDEC ATTN: SMCAR-IMI-I Picatinny Arsenal, NJ 07806-5000	(Under class only) 1	Commandant US Army Infantry School ATTN: ATSH-CD-CSO-OR Fort Benning, GA 31905-5660
2	Commander US Army, ARDEC ATTN: SMCAR-TDC Picatinny Arsenal, NJ 07806-5000	1	Air Force Armament Laboratory ATTN: AFATL/DLODL Eglin AFB, FL 32542-5000
1	Director Benet Weapons Laboratory US Army, ARDEC ATTN: SMCAR-CCB-TL Watervliet, NY 12189-4050		<u>Aberdeen Proving Ground</u>
1	Commander US Army Armament, Munitions and Chemical Command ATTN: SMCAR-ESP-L Rock Island, IL 61299-5000	2	Dir. USAMSA ATTN: AMXSY-D AMXSY-MP, H. Cohen
1	Commander US Army Aviation Systems Command ATTN: AMSAV-DACL 4300 Goodfellow Blvd. St. Louis, MO 63120-1798	1	Cdr. USATECOM ATTN: AMSTE-TD
		3	Cdr. CRDEC, AMCCOM ATTN: SMCCR-RSP-A SMCCR-MU SMCCR-MSI
		1	Dir. VIAMO ATTN: AMSLC-VL-D

No. of

Copies Organization

- 1 National Research Council
Office of Scientific and Engineering
Personnel
ATTN: Dr. Arnold E. Schwartz
2101 Constitution Avenue
Washington, DC 20418
- 1 Orlando Technologies, Incorporated
ATTN: Dr. Daniel A. Manuska
P.O. Box 855
Shalimar, FL 32579
- 2 Science Applications International
Corporation
ATTN: Dr. Jad H. Bateh
Mr. Lindsey Thornhill
1503 Johnson Ferry Road
Marietta, GA 30062
- 2 Science Applications International
Corporation
ATTN: Dr. Keith A. Jamison
Dr. Glenn E. Kolader
1247-B North Eglin Parkway
Shalimar, FL 32579
- 1 Science Applications International
Corporation
ATTN: Dr. A.J. Toepfer
2109 Air Park Road, S.E.
Albuquerque, NM 87122
- 1 TITAN Spectron Division
ATTN: Dr. Bruce R. Miller
2340 Alamo Boulevard, S.E.
Suite 200
Albuquerque, NM 87106
- 1 Georgia Institute of Technology
ATTN: Dr. P.V. Desai
Department of Mechanical Engineering
Atlanta, GA 30332
- 1 University of Miami
ATTN: Dr. Manuel A. Huerta
Physics Department
P.O. Box 248046
Coral Gables, FL 33124

USER EVALUATION SHEET/CHANGE OF ADDRESS

This Laboratory undertakes a continuing effort to improve the quality of the reports it publishes. Your comments/answers to the items/questions below will aid us in our efforts.

1. BRL Report Number BRL-TR-3108 Date of Report JUNE 1990

2. Date Report Received _____

3. Does this report satisfy a need? (Comment on purpose, related project, or other area of interest for which the report will be used.)

4. Specifically, how is the report being used? (Information source, design data, procedure, source of ideas, etc.)

5. Has the information in this report led to any quantitative savings as far as man-hours or dollars saved, operating costs avoided, or efficiencies achieved, etc? If so, please elaborate.

6. General Comments. What do you think should be changed to improve future reports? (Indicate changes to organization, technical content, format, etc.)

CURRENT ADDRESS Name _____

 Organization _____

 Address _____

 City, State, Zip Code _____

7. If indicating a Change of Address or Address Correction, please provide the New or Correct Address in Block 6 above and the Old or Incorrect address below.

OLD ADDRESS Name _____

 Organization _____

 Address _____

 City, State, Zip Code _____

(Remove this sheet, fold as indicated, staple or tape closed, and mail.)

.....FOLD HERE.....

DEPARTMENT OF THE ARMY

Director
U.S. Army Ballistic Research Laboratory
ATTN: SLCBR-DD-T
Aberdeen Proving Ground, MD 21005-5066

OFFICIAL BUSINESS



NO POSTAGE
NECESSARY
IF MAILED
IN THE
UNITED STATES

BUSINESS REPLY MAIL
FIRST CLASS PERMIT No 0001, APG, MD

POSTAGE WILL BE PAID BY ADDRESSEE

Director
U.S. Army Ballistic Research Laboratory
ATTN: SLCBR-DD-T
Aberdeen Proving Ground, MD 21005-9989

.....FOLD HERE.....